Published in final edited form as:
Nat Methods. 2018 March ; 15(3): 183–186. doi:10.1038/nmeth.4579.

EVIR: Chimeric receptors that enhance dendritic cell cross-dressing with tumor antigens

Mario Leonardo Squadrito[1], **Chiara Cianciaruso**[1], **Sarah K. Hansen**[1], and **Michele De Palma**[1]

[1]Swiss Institute for Experimental Cancer Research (ISREC), School of Life Sciences, École Polytechnique Fédérale de Lausanne (EPFL), 1015 Lausanne, Switzerland

Abstract

We describe a lentivirus-encoded chimeric receptor, termed extracellular vesicle (EV)-internalizing receptor (EVIR), which enables the selective uptake of cancer cell-derived EVs by dendritic cells (DCs). The EVIR enhances DC presentation of EV-associated tumor antigens to $CD8^+$ T cells primarily through MHCI recycling and cross-dressing. EVIR-engineered DCs may increase the applications of DC-based cancer vaccines.

Virtually all cell types produce EVs encompassing exosomes and other microvesicles1, 2. Tumor-derived EVs modulate cancer-associated processes, such as immunity and metastasis, by interacting with various cell types, both locally in the tumor microenvironment and via the systemic circulation in remote organs2, 3. EVs may also deliver tumor antigens (TAs) to dendritic cells (DCs); however, the mechanistic underpinnings of this phenomenon are poorly understood4–7.

In order to examine the process of EV-mediated TA transfer to DCs, we designed a chimeric receptor, termed EVIR, which endows DCs with the capacity to specifically recognize cancer cell-derived EVs. The EVIR encompasses a truncated (non-signaling) low-affinity nerve growth factor receptor (dLNGFR) and an extracellular antibody domain (Fig. 1a). The latter comprises an IgK signal peptide and a single-chain $F(ab')_2$ variable fragment (scFv) with specificity for the human HER2 protein, which is overexpressed in a subset of human breast cancers8. A hinge domain derived from dLNGFR connects the transmembrane and extracellular domains of the EVIR. We also generated a non-functional EVIR lacking the scFv domain, hereon referred to as control receptor (CtrlR).

Correspondence: M.L.S. (mario.squadrito@epfl.ch) and M.D.P. (michele.depalma@epfl.ch).

Author contributions

M.L.S. constructed LVs, designed and performed research, analyzed and interpreted the data, assembled the display items, and wrote the manuscript. C.C. designed and analyzed EV internalization and MHCI recycling assays, and contributed to the writing of the manuscript. S.K.H. performed some experiments. M.D.P. designed and coordinated research, interpreted the data, and wrote the manuscript.

Competing financial interests

M.L.S. and M.D.P. are inventors of a patent application filed by EPFL, which describes the EVIR technology.

Europe PMC Funders Author Manuscripts

We used a bidirectional lentiviral vector (LV) (Ref 9) to coordinately express the EVIR (or CtrlR) and a green fluorescent protein (GFP) transgene (Supplementary Fig. 1a). Anti-scFv staining of immortalized mouse bone marrow macrophages (iBMMs) (Ref 10) transduced with the EVIR-encoding LV (iBMM-EVIR) showed efficient and sustained cell surface expression of the EVIR (Fig. 1b and Supplementary Fig. 1b).

In a cell-suspension assay, mouse P388D1 monocytes transduced with the EVIR (Mo-EVIR) readily adhered to $HER2^+$, but not HER2-negative, MC38 colorectal cancer cells fluorescently labeled with mCherry (MC38-HER2/mCh and MC38-mCh, respectively; Fig. 1c and Supplementary Fig. 1c, d). We observed cell aggregation also when we cultured iBMM-EVIR with $HER2^+$ MC38 cells for 24 h under adherent conditions (Supplementary Fig. 1c, e). Of note, the aggregation of MC38-HER2 (labeled with mTurquoise2, mTq) and iBMM-EVIR (labeled with GFP) did not promote the unspecific co-aggregation of iBMM (labeled with mCh) in mixed cultures. Thus, an anti-HER2 EVIR specifically and efficiently binds to HER2 expressed on the surface of cancer cells.

To examine whether the EVIR enhances the uptake of $HER2^+$ EVs by BM-derived DCs (BMDCs), we exposed EVIR- and CtrlR-expressing DCs (DC-EVIR and DC-CtrlR, respectively; Supplementary Fig. 2a) to EVs isolated from either $HER2^+$ or HER2-negative MC38-mCh cells (EV-HER2/mCh and EV-mCh, respectively; Supplementary Fig. 2b-c). EV-HER2/mCh transferred mCh fluorescence to DC-EVIR more efficiently than EV-mCh (Fig. 1d). Moreover, DC-EVIR acquired mCh fluorescence from EV-HER2/mCh more efficiently than DC-CtrlR (Fig. 1e; Supplementary Fig. 2d, e). Over time, the mCh fluorescence pattern transitioned from membrane-associated, to largely punctate in the cytoplasm, to broadly diffuse in the cytoplasm; this kinetics appeared faster in DC-EVIR (Supplementary Fig. 3a). Furthermore, matched amounts of EVs isolated from MC38-mTq cells (EV-mTq) did not impair the ability of iBMM-EVIR to acquire mCh fluorescence from EV-HER2/mCh (Supplementary Fig. 3b), suggesting that an anti-HER2 EVIR can efficiently bind to, and internalize, EV-HER2 also in the presence of competing doses of HER2-negative EVs.

To investigate whether the anti-HER2 EVIR improves the presentation of TAs by DCs, we performed T-cell proliferation assays. We cultured $CD8^+$ OT-I T cells, which recognize the chicken ovalbumin (OVA)-derived SIINFEKL peptide loaded onto H-2Kb/B2M major histocompatibility class I (MHCI) complex11, with either DC-EVIR or DC-CtrlR that had been pre-incubated with EVs isolated from $HER2^+$ or negative MC38 cells expressing OVA (EV-HER2/OVA and EV-OVA, respectively). EV-HER2/OVA greatly enhanced the proliferation of $CD8^+$ OT-I cells co-cultured with DC-EVIR cells, compared to the other conditions (Fig. 1f and Supplementary Fig. 4a). Of note, we did not observe T-cell proliferation in response to EV-HER2/OVA in the absence of DCs. T-cell proliferation induced by DC-EVIR plateaued at lower EV-HER2/OVA doses, compared to DC-CtrlR (Supplementary Fig. 4b). Thus, the anti-HER2 EVIR enhances MHCI-mediated presentation of a surrogate TA contained in HER2-positive EVs.

Cross-dressing defines the acquisition by DCs of MHCI/antigen complexes shed by other cells12, 13. We asked whether the EVIR enhances TA presentation preferentially through

classical TA internalization, processing and cross-presentation14, or by promoting DC cross-dressing with EV-associated, pre-formed MHCI/antigen complexes. We deleted the MHCI subunit *B2m,* common to all MHCI complexes, or *H2kb*, which is specific for the SIINFEKL peptide, in both MC38-HER2/OVA and MC38-OVA cells using a LV-based CRISPR-Cas9 strategy (Supplementary Fig. 5a-b). Both *B2m* and *H2kb* knockout (KO) cells had an intact OVA transgene (Supplementary Fig. 5c) and released EVs that were comparable, according to abundance and size distribution, to those of unmodified cells (Supplementary Fig. 5d). Also, we did not observe differences between EVs isolated from *B2m* or *H2kb*-deficient and proficient (unmodified) cells when we analyzed EV internalization by DCs (Supplementary Fig. 5e).

Unexpectedly, DC-EVIR failed to promote $CD8^+$ OT-I T-cell proliferation in the presence of EVs isolated from either *H2kb or B2m* KO cancer cells (Fig. 2a and Supplementary Fig. 6a), suggesting that MHCI/antigen complexes carried by EVs are required to stimulate OVA-specific T-cell proliferation. To further validate these results, we generated BMDCs from *B2m* KO mice15 and found that the lack of endogenous MHCI/SIINFEKL complexes on the DCs (Supplementary Fig. 6b) did not prohibit EVIR-mediated enhancement of T-cell proliferation in the presence of EV-HER2/OVA (Fig. 2b). Mass-spectrometry analysis indicated that MC38-derived EVs contain H-2Kb (Supplementary Table 1), supporting a mechanism of horizontal transfer of H-2Kb from the EVs to the DCs.

In order to analyze EV-mediated H-2Kb transfer, we used DCs generated from FVB/n mice, which lack H-2Kb (Supplementary Fig. 6c). In this setting, EV-HER2/OVA transferred H-2Kb to $H\text{-}2Kb^-$ DCs in an EVIR-dependent manner (Supplementary Fig. 6d). Moreover, $H\text{-}2Kb^+$ MC38-HER2/GFP cells efficiently transferred H-2Kb to $H\text{-}2Kb^-$ DC-EVIR in a DC/cancer cell co-mingling assay performed in immunodeficient NSG mice (Supplementary Fig. 7a-d), which also lack endogenous H-2Kb MHCI (Supplementary Fig. 6c). Collectively, these data indicate that the EVIR enables TA presentation largely by cross-dressing DCs with EV-derived MHCI/antigen complexes.

We then studied the mechanism of MHCI transfer to DCs. PKH67-labelled $HER2^+$ EVs (EV-HER2/PKH67) were protected from trypsin/acid digestion as early as 2 h after incubation with DC-EVIR, indicative of rapid EV internalization (Supplementary Fig. 8a). Two macropinocytosis/phagocytosis inhibitors, amiloride and cytochalasin-D, blocked EV internalization, whereas an inhibitor of clathrin-mediated endocytosis had only modest effects on EV internalization (Supplementary Fig. 8b). Accordingly, EV-HER2/PKH67 that had been internalized by DC-EVIR largely co-localized with fluorescently labeled dextran, which is internalized through a macropinocytosis-dependent endocytic pathway, but not with transferrin, which is internalized through receptor-dependent, clathrin-mediated endocytosis (Supplementary Fig. 8c). Of note, EV-HER2/PKH67 that had been internalized by DC-CtrlR did not seem to specifically associate with dextran, suggesting that the EVIR enhanced EV internalization via macropinocytosis.

We then used EV-HER2/mCh to trace the fate of the EVs following internalization by DCs (Supplementary Fig. 9a-d). As early as 1 h after EV incubation with DCs, the mCh signal co-localized with $EEA1^+$ early endosomes in both DC-EVIR and DC-CtrlR. At 5 h, mCh

co-localized with both RAB11$^+$ recycling endosomes and LAMP1$^+$ lysosomes; however, DC-EVIR showed enhanced sorting to recycling endosomes and decreased sorting to lysosomes compared to DC-CtrlR. These results suggest that the EVIR encourages the shunting of EV cargo from degradation to recycling, a process that may account for EVIR-mediated MHCI cross-dressing. To extend these findings, we also analyzed the kinetics of H-2Kb internalization and recycling in H-2Kb$^-$ DC-EVIR that had been exposed to H-2Kb$^+$ EV-HER2/PKH67 (Fig. 2c and Supplementary Fig. 10). Most of the H-2Kb co-localized with internalized EVs at 5 h, consistent with the expected kinetics of EV endocytosis. However, H-2Kb co-localization with the plasma membrane became evident at 24 h. These results strongly argue that EVIR-engineered DCs can internalize and recycle functional MHCI-peptide complexes by adsorbing tumor-derived EVs.

To explore the versatility of the EVIR platform, we designed an EVIR specific for the disialoganglioside GD2, which is highly expressed in human melanoma16. In order to obtain GD2-expressing cancer cells, we transduced MC38-mCh cells with LVs encoding for the GD2 synthases GD2S and GD3S (Ref 17). This resulted in robust GD2 expression by non-melanoma MC38-mCh cells (Supplementary Fig. 11a). Expression of the anti-GD2 EVIR in iBMMs enhanced their ability to acquire mCh fluorescence from EVs isolated from GD2$^+$ MC38-mCh cells (Supplementary Fig. 11b).

We also examined CD8$^+$ OT-I cell proliferation in response to GD2$^+$ melanoma-derived EVs and anti-GD2 EVIR-transduced DCs. For these experiments, we engineered the OVA-positive mouse melanoma cell line SM1-OVA to express GD2 (Supplementary Fig. 11c). Because cross-dressing requires MHCI expression in the cancer cells, we stimulated MHCI expression in SM1-OVA cells with interferon-γ (IFNγ; Supplementary Fig. 11d). We then co-cultured CD8$^+$ OT-I cells with either DC-EVIR or DC-CtrlR, and treated the co-culture with EVs isolated from either IFNγ-treated or untreated SM1-GD2/OVA cells (EV-SM1-GD2/OVA^{IFN} and EV-SM1-GD2/OVA, respectively; Supplementary Fig. 11e). In the presence of EV-SM1-GD2/OVA^{IFN}, the DC-EVIR cells enhanced CD8$^+$ OT-I cell proliferation compared to DC-CtrlR (Supplementary Fig. 11f). Conversely, EV-SM1-GD2 did not stimulate OT-I cell proliferation, likely because of the low amounts of MHCI/peptide complexes on the surface of these EVs. These results provide further evidence that EVIRs can be broadly used to stimulate TA-specific T-cell responses through DC cross-dressing.

To examine if DC-EVIR can potentiate an antigen-specific anti-tumoral immune response, we inoculated MC38-HER2 cells subcutaneously in syngenic mice and, when the tumors were established, vaccinated the mice with either anti-HER2 DC-EVIR or DC-CtrlR cells. Vaccination with DC-EVIR inhibited MC38-HER2 tumor growth more efficiently than vaccination with DC-CtrlR (Fig. 2d). In an independent experiment that used MC38-HER2/OVA cells, we observed a small but statistically significant expansion of endogenous, tumor-specific CD8$^+$ T cells in the spleen of mice that had been vaccinated with DC-EVIR, compared to DC-CtrlR (Fig. 2e; Supplementary Fig. 12). These data suggest that EVIR-engineered DCs can promote anti-tumoral responses by harnessing tumor-derived EVs and their cargo of TAs.

In summary, EVIR chimeric receptors enable the specific and efficient uptake of cancer cell-derived EVs by antigen-presenting cells. Our results emphasize the significance of DC cross-dressing with pre-formed MHCI/TA complexes for the activation of TA-specific specific T-cell responses. The EVIR platform may be exploited for identifying EV-associated TAs and cognate T cell receptors (TCR) through *ex vivo* cells assays, or for enhancing the priming of $CD8^+$ T cells toward unknown, patient- and tumor-specific TAs in therapeutic DC vaccination settings. In the future, DC-EVIR vaccination may be combined with strategies that enhance T cell activation and alleviate cancer-associated immunosuppression, such as through vascular reprogramming, macrophage depletion, or immune checkpoint blockade18, 19.

Online Methods

Design and construction of lentiviral vectors (LVs) encoding EVIRs

In order to generate an anti-HER2 EVIR, a mouse-optimized DNA sequence coding for the CHA21 scFv, designed according to a previous study20, was obtained from GeneArt® (Life Technologies). A DNA sequence coding for the IgK signal peptide (MDFQVQIFSFLLISASVIMSRG) was incorporated at the 5’-end of the CHA21 sequence to enable the export of the receptor to the cell membrane**.** A DNA sequence containing a high efficiency Kozak sequence and a BamHI restriction site were incorporated at the 5’-end of the CHA21-IgK DNA sequence. We also inserted a DNA sequence containing AgeI, MluI and XhoI restriction sites, and a stop codon (TGA), at the 3’-end of the CHA21-IgK coding sequence.

The synthetic DNA sequence encoding the IgK-CHA21 construct was then inserted in a LV plasmid downstream to a spleen forming focus virus (SFFV) promoter and upstream to the WPRE stabilizing sequence21 by using the BamHI and SalI restriction sites of the plasmid.

A human truncated low-affinity nerve growth factor receptor (dLNGFR), comprising the intracellular (IC) domain, the transmembrane (TM) domain, and a segment of the extracellular (EC) domain, was obtained by polymerase chain reaction (PCR) from a plasmid containing a dLNGFR sequence21 using the following primers containing AgeI and MluI restriction sites:

Fw (AgeI): AAAAAACCGGTCTTCTGGGGGTGTCCCTTG;

Rv (Mlu): AAAAAACGCGTAGTTAGCCTCCCCCATCTCC.

The PCR product was then cloned using AgeI and MluI restriction sites downstream to the CHA21 sequence and upstream to the stop codon in the SFFV.IgK-CHA21.WPRE plasmid, producing the SFFV.EVIR.WPRE LV.

In order to enable tracing of EVIR expression, the SFFV.EVIR.WPRE sequence was cloned into a bidirectional LV22 by replacing the human PGK (hPGK).dLNGFR cassette with the SFFV.EVIR cassette using EcoRV and AvrII restriction sites. In this bidirectional LV, the GFP is expressed under the transcriptional control of the minimal cytomegalovirus promoter (mCMV). The full amino acid sequence of the anti-HER2 EVIR is as follows:

>anti-HER2_EVIR

MDFQVQIFSFLLISASVIMSRGDIVLTQTPSSLPVSVGEKVTMTCKSSQTLLYSNNQK
NYLAWYQQKPGQSPKLLISWAFTRKSGVPDRFTGSGSGTDFTLTIGSVKAEDLAVYY
CQQYSNYPWTFGGGTRLEIKRGGGGSGGGGSGGGGSGGGGSEVQLQQSGPEVVKT
GASVKISCKASGYSFTGYFINWVKKNSGKSPEWIGHISSSYATSTYNQKFKNKAAFT
VDTSSSTAFMQLNSLTSEDSAVYYCVRSGNYEEYAMDYWGQGTSVTVSSTGLLGVS
LGGAKEACPTGLYTHSGECCKACNLGEGVAQPCGANQTVCEPCLDSVTFSDVVSAT
EPCKPCTECVGLQSMSAPCVEADDAVCRCAYGYYQDETTGRCEACRVCEAGSGLVF
SCQDKQNTVCEECPDGTYSDEANHVDPCLPCTVCEDTERQLRECTRWADAECEEIP
GRWITRSTPPEGSDSTAPSTQEPEAPPEQDLIASTVAGVVTTVMGSSQPVVTRGTTDN
LIPVYCSILAAVVVGLVAYIAFKRWNRGIL

In order to generate an anti-GD2 EVIR, a mouse-optimized anti-GD2 14.G2a scFv sequence, designed according to a previous study23, was obtained from GeneArt®. Construction of this EVIR used molecular cloning steps that were analogous to those used for constructing the anti-HER EVIR. Briefly, a sequence coding for the IgK signal peptide (described above) was cloned at the 5'-end of the 14.G2a sequence. A DNA sequence containing a high efficiency Kozak sequence and a BamHI restriction site were incorporated at the 5'-end of the 14.G2a scFv coding sequence, as described above. A restriction site for AgeI was incorporated at the 3'-end of the scFv. The CHA21-IgK sequence in the SFFV.EVIR.WPRE LV was then replaced with the 14G.2a-IgK sequence. The resulting SFFV.EVIR.WPRE sequence was cloned into the bidirectional LV described above. The full amino acid sequence of the anti-GD2 EVIR is as follows:

>anti-GD2_EVIR

MDFQVQIFSFLLISASVIMSRGEVQLLQSGPELEKPGASVMISCKASGSSFTGYNMN
WVRQNIGKSLEWIGAIDPYYGGTSYNQKFKGRATLTVDKSSSTAYMHLKSLTSEDSA
VYYCVSGMEYWGQGTSVTVSSGGGGSGGGGSGGGGSDVVMTQTPLSLPVSLGDQ
ASISCRSSQSLVHRNGNTYLHWYLQKPGQSPKLLIHKVSNRFSGVPDRFSGSGSGTD
FTLKISRVEAEDLGVYFCSQSTHVPPLTFGAGTKLELTGLLGVSLGGAKEACPTGLYT
HSGECCKACNLGEGVAQPCGANQTVCEPCLDSVTFSDVVSATEPCKPCTECVGLQS
MSAPCVEADDAVCRCAYGYYQDETTGRCEACRVCEAGSGLVFSCQDKQNTVCEEC
PDGTYSDEANHVDPCLPCTVCEDTERQLRECTRWADAECEEIPGRWITRSTPPEGSD
STAPSTQEPEAPPEQDLIASTVAGVVTTVMGSSQPVVTRGTTDNLIPVYCSILAAVVV
GLVAYIAFKRWNRGIL

The CtrlR-expressing LV was obtained by cloning the dLNGFR sequence without the scFv sequence in the SFFV.WPRE LV using BamHI and SalI restriction enzymes. The resulting SFFV.CtrlR.WPRE sequence was then cloned in the bidirectional LV described above.

Construction of LVs encoding other transgenes

In order to express mTurquoise2 (mTq), we generated a CMV.mTq.WPRE LV by replacing the GFP sequence in the CMV.GFP.WPRE LV, described previously 21, with the mTq

coding sequence24 (a gift of Antoine Royant, Institut de Biologie Structurale, Grenoble, France), using BamHI and SalI restriction sites.

In order to express HER2 in cancer cells, we generated a hPGK.HER2.WPRE LV by replacing the mCherry (mCh) coding sequence in the hPGK.mCh.WPRE LV, described previously25, with a human HER2 coding sequence26, provided by Livio Trusolino (University of Torino Medical School, Italy), using BamHI and SalI restriction sites.

In order to express GD2 in cancer cells, we generated two LVs, hPGK.GD2S.WPRE and hPGK.GD3S.WPRE, by replacing the *HER2* coding sequence in the LV described above with mouse-optimized sequences encoding GD2 synthase (NCBI accession: NM_027739) or GD3 synthase (NCBI accession: NM_011374), respectively, obtained from GeneArt®, using BamHI and SalI restriction sites.

In order to disrupt *H2kb* or *B2m* in MC38 cells, we generated self-inducible CRISPR/Cas9-based LVs. We obtained a LV containing both a TetO-CAS9 expression cassette and a hPGK promoter-regulated bicistronic cassette for the expression of the reverse tTA (rtTA) and puromycin (PURO) (a gift of Angelo Lombardo, San Raffaele Scientific Institute, Milan, Italy). We then obtained from GeneArt® a DNA sequence containing a U6-driven gRNA hosting a BsmBI cloning site for rapid and one-step annealing and ligation of crRNA sequences against the gene of interest. We cloned the U6-gRNA cassette upstream to the TetO-CAS9 expression cassette using ClaI and XhoI restriction sites, to obtain the doxycycline-self-inducible U6-sgRNA.TetO-CAS9.hPGK-PURO/2A/rtTA LV (shown in Supplementary Figure 5a). In order to employ the ClaI restriction site, the U6-sgRNA.TetO-CAS9.hPGK-PURO/2A/rtTA plasmid was expanded and isolated in the *dam*-deficient *E. coli* strain GM2163. We then sought to remove BsmBI restriction sites interfering with the process of one-step cloning. To this aim, we replaced the hPGK and PURO sequences in the parental plasmid with mutated hPGK and PURO sequences obtained from GeneArt®. Both mutated sequences were cloned in the U6-sgRNA.TetO-CAS9.hPGK-PURO/2A/rtTA LV using BamHI and XbaI restriction sites. We then annealed and ligated the DNA oligos shown below using the BsmBI restriction site of the U6-sgRNA.TetO-CAS9.hPGK-PURO/2A/rtTA LV.

gRNA sequences:

Control gRNA: GCGAGACGACCATGGACGTCTCC

H2kb gRNA: GGGCCCGGTACTCACCCGCG

B2m gRNA: GGTCGTCAGCATGGCTCGCT

Oligos to generate genome-targeting gRNAs:

gR_*H2k1*_1_Se: ACCGGGCCCGGTACTCACCCGCG

gR_*H2k1*_1_AS: AAACCGCGGGTGAGTACCGGGCC

gR_*B2m*_1_Se: ACCGGTCGTCAGCATGGCTCGCT

gR_*B2m*_1_AS: AAACAGCGAGCCATGCTGACGAC

Cell lines and primary cell cultures

Immortalized murine bone marrow derived macrophages (iBMM) were described previously25. iBMMs were cultured in Iscove's Modified Dulbecco's Medium (IMDM, Sigma), supplemented with mouse colony-stimulating factor-1 (CSF1, 50 ng/ml, Peprotech), L-glutamine and penicillin-streptomycin (Life Technologies), and 20% fetal bovine serum (FBS; EuroClone Group).

Murine P388D1 monocytic cells, MC38 and MC38-OVA colon carcinoma cells (provided by Nicole Haynes, Peter MacCallum Cancer Center, Melbourne), SM1-OVA melanoma cells (provided by Antony Ribas, University of California, Los Angeles, CA), and human 293T embryonic kidney cells, were cultured in IMDM supplemented with 10% FBS, glutamine and penicillin-streptomycin. In some experiments, SM1-OVA cells were stimulated with interferon-γ (IFNγ; Peprotech) for 24 h before use.

Bone marrow (BM) cells were obtained by flashing femurs and tibiae of 6-8 week old wild-type (C57Bl/6 or FVB/n) or *B2m* KO (C57Bl/6) mice27 with ice-cold PBS. BM cells of *B2m*-deficient mice were a gift of Greta Guarda (University of Lausanne, Switzerland). In order to generate dendritic cells (DCs), BM cells were cultured for 7-8 days in RPMI medium supplemented with GM-CSF (100 ng/ml, Peprotech) and IL4 (40 ng/ml, Peprotech), 10% FBS, glutamine and penicillin-streptomycin.

LV production

Vesicular stomatitis virus (VSV)-pseudotyped, third-generation LVs were produced by transient five-plasmid co-transfection into 293T cells, as described previously28, with some modifications. Briefly, 9 million 293T cells were seeded in 15 cm dishes 24 h before transient transfection in 20 ml of cell culture medium. For each dish, a plasmid mix was prepared containing (i) the envelope plasmid (VSV-G, 9 μg), (ii) the packaging pMDLg/pRRE plasmid (12.5 μg), (iii) the REV plasmid (6.25 μg), (iv) the pADVANTAGE plasmid (15 μg), and (v) the transfer lentiviral plasmid (32 μg). Transient transfection was performed as described previously28. After 30 h, the cell supernatant was collected, filtered (0.22 μm), and concentrated by ultracentrifugation using a Beckman ultracentrifuge equipped with a SW32Ti rotor, at 82'600 RCF for 2h at 20°C. LV particles were collected in PBS and stored at –80ºC.

LVs were titred using 293T cells. The percentage of marker (dLNGFR, HER2, GFP, mCh, or mTq)-positive cells was measured by flow cytometry 4-7 days after transduction, and the titer calculated as described previously28. The titers of LVs used to express GD2S, GD3S and the CRISPR/Cas9-based system were calculated by measuring the copy number of vector integrated per genome by quantitative PCR, as described previously28. We obtained titers ranging from 10^9 to 10^{10} transducing units (TU)/ml after LV ultracentrifugation.

Europe PMC Funders Author Manuscripts

Europe PMC Funders Author Manuscripts

Cell transduction

Stable cell lines (MC38, MC38-OVA, SM1-OVA, P388D1, and iBMM) cells were transduced with LV doses ranging from multiplicity of infection (MOI) 5 to 10. In experiments with double transduction, the cells were transduced sequentially, one day apart. Transduced cells were propagated for several days or weeks, and stored at –80ºC.

To transduce primary BM-derived DCs, BM cells were transduced with a LV dose of 100 MOI, 2 days after seeding in RPMI supplemented with GM-CSF and IL4. Twenty-four hours post-transduction, transduced BM cells were washed and seeded for DC differentiation in the presence of GM-CSF and IL4 for at least 5-6 days before use.

Cell-binding assays

We performed cell-binding assays in cell suspension conditions. Transduced P388D1 monocytes (Mo-EVIR and Mo-CtrlR) were incubated with MC38-HER2/mCh (or control MC38-mCh) cancer cells as follows. MC38 cells were detached by trypsin/EDTA, whereas P388D1 cells were detached by pipetting. After washing in PBS, MC38 and P388D1 cells were co-incubated at either 1:1, 9:1 or 1:9 ratio in 100 µl of PBS at a concentration of 10^7 cells/ml at 4°C in a spinning wheel for 20 min. Cells were immediately analyzed by flow cytometry or confocal microscopy (see below).

We performed cell-binding assays in cell adhesion conditions. We seeded $2x10^4$ MC38-HER2/mTq (or control MC38-mTq) cancer cells in 24-well plates (Corning). One h later, we seeded iBMM-EVIR, iBMM-CtrlR or iBMM-mCh cells on the cancer cells, at 1:1 ratio. After 24 h of co-culture, cells were detached by a short incubation with trypsin/EDTA (3 min at 37°C), washed with wash solution (PBS, 4 mM EDTA and 1% FBS), resuspended in wash solution containing 7-aminoactinomycin-D (7AAD, Sigma) to exclude dead cells, and immediately analyzed by flow cytometry (see below).

EV isolation, quantification, and labeling with PKH67

In order to isolate EVs, MC38, MC38-OVA or SM1-OVA cells were cultured for at least 3 days in RPMI medium supplemented with FBS depleted of EVs by ultracentrifugation at 134’000 RCF for 6 h. The cell culture medium was centrifuged at 500 RCF for 5 min; 2000 RCF for 5 min; and finally at 4600 RCF for 20 min at 4°C to remove cells and debris. The resulting medium was then ultracentrifuged at 134’000 RCF for 70 min at 4°C using a Beckman ultracentrifuge and a SW32Ti rotor. EVs were resuspended in PBS and stored at –80°C.

The size and concentration of the EV particles was determined by nanoparticle tracking analysis (NTA) using a Nanosight NS300 device (Malvern Instruments, UK). Typically, purified EVs were diluted 1:100 or 1:1000 in PBS prior to analysis. Three measurements of 60 sec were recorded for each sample.

EV labeling with PKH67 was performed by modifying the manufacturer’s protocol (Sigma). Briefly, the EV preparations were diluted in diluent C prior to addition of PKH67 (1 µl per 100 µl of solution). Labeling was performed for 10 min at room temperature in the dark and terminated using 0.5% BSA (Sigma). EVs were washed twice with PBS and concentrated by

ultracentrifugation, as described above. The pellet was resuspended in PBS and stored at –80°C. As a negative control for immunofluorescence studies, we diluted PKH67 in PBS and processed it by ultracentrifugation as described above.

Liquid chromatography-tandem mass spectrometry (LC-MS/MS) of EVs

EVs (10 μg of total protein, quantified by BCA protein assay kit; Thermo Fisher) were obtained from MC38 cells, as described above. The sample was processed as previously described29. Peptides were desalted using StageTips and dried in a vacuum concentrator. For LC-MS/MS analysis, the peptides were separated by reverse phase chromatography on a Dionex Ultimate 3000 RSLC nano UPLC system connected in-line with an Orbitrap Elite (Thermo Fisher Scientific). Database search was performed using Mascot 2.5 (Matrix Science) and SEQUEST in Proteome Discoverer v.1.4. against a murine Uniprot protein database. Data were further processed and inspected in ScaffoldTM 4.8.4 (Proteome Software). Two independent analyses were performed on one EV preparation.

Immunofluorescence analysis of transduced iBMMs

iBMMs were seeded on 8-well glass chamber slides (Corning) coated with fibronectin (200 μg/ml, Peprotech), at a concentration of 2 x 10^4 cells/well. To visualize the EVIR, the cells were stained with a directly conjugated anti-F(ab')2 antibody (see Supplementary Table 3 for details) and phalloidin-AlexaFluor-546 (Life technologies), in the absence of blocking solution, followed by DAPI staining. After staining, the cells were washed, fixed, and processed for confocal microscopy as described below.

Immunofluorescence analysis of EV-treated DCs

BM-derived DCs were seeded on 8 mm round glass coverslips coated with poly-D-lysine (50 μg/ml, Sigma) in 48-well plates (Corning), at a concentration of about 1.25 x 10^5 cells/ml. The cells were incubated with EVs either containing mCh or pre-labeled with PKH67 (2x10^8 EVs/well according to NTA analysis, unless indicated otherwise) for the time specified in the figure legends. After cell incubation with the EVs, the cells were washed, fixed, and processed for confocal microscopy as described below.

DC treatment with tracers or inhibitors of endocytosis

In order to trace macropinocytosis and clathrin-mediated endocytosis, 70 kD TRITC-conjugated dextran (Sigma) or AlexaFluor-555–conjugated transferrin (Life Technologies) were respectively added (both at 30 μg/ml) to the DCs 5 min prior to incubation with PKH67-labeled EVs. After 2 h, the DCs were fixed and analyzed by immunofluorescence staining, as described below.

In order to inhibit endocytosis, the DCs were treated with 1 μM cytochalasin-D (Sigma), 10 μM chlorpromazine (Sigma), or 150 μM 5-(N-Ethyl-N-isopropyl) amiloride (Sigma), which are non-specific inhibitors of phagocytosis/macropinocytosis, chlatrin-mediated endocytosis (CME), and macropinocytosis, respectively, for 30 min prior to incubation with PKH67-labeled EVs. After 2 h, the DCs were fixed and analyzed by immunofluorescence staining, as described below.

Preparation of iBMMs and DCs for confocal microscopy

At the end of the experiments, the cells were fixed in 4% in paraformaldehyde (PFA) for 15 min at room temperature in the dark. After removing the PFA, the cells were incubated for 30 min in blocking solution containing 0.3% Triton, 10% normal goat serum (NGS) and an anti-CD16/CD32 Fc receptor-blocking antibody (Fc block; see Supplementary Table 3 for details) in PBS. Following immunofluorescence staining (see below), the slides were washed with PBS and stained with 4',6-diamidino-2-phenylindole (DAPI, 1 μg/ml; Sigma) to reveal cell nuclei. The glass coverslips were mounted in Dako mounting medium (Agilent), dried overnight at room temperature, and analyzed by a confocal microscope.

Immunofluorescence staining of endosomal proteins

In order to visualize endosomal proteins, a staining solution was prepared by diluting the primary antibodies (anti-EEA1, anti-RAB11, or anti-LAMP1, along with directly-conjugated anti-LNGFR; see Supplementary Table 3 for details) in blocking solution. The staining solution was added (120 μl per well) for an overnight incubation at 4°C. After washing, secondary antibodies (see Supplementary Table 3 for details) were added for 30 min in PBS containing 0.3% Triton. In all immunofluorescence imaging experiments, mCh was detected using a chicken anti-mCh primary antibody followed by AlexaFluor-555-conjugated anti-chicken secondary antibody.

Immunofluorescence staining of intracellular H-2Kb

For intracellular H-2Kb staining and confocal imaging, we used a modified protocol. Live cells were washed in blocking solution and then fixed with Fix/Perm solution (using the FOXP3 staining kit for flow cytometry; eBioscience) for 20 min on ice. After washes with PBS, the cells were incubated with a PE-conjugated anti-H-2Kb antibody for 30 min, washed extensively, fixed with 4% PFA, and processed for further staining as described above.

Image analysis by confocal microscopy

After image acquisition using a confocal microscope (Zeiss LSM 700), the images were processed and analyzed with ImageJ (NIH). Transduced cells were identified by the presence of membrane-associated dLNGFR.

The intracellular localization of the mCh signal was analyzed by quantifying the amount of mCh signal showing: (i) a punctate pattern associated to the plasma membrane; (ii) a punctate pattern inside the cell; or (iii) an intracellular diffuse pattern. Analysis of EV internalization was performed by measuring the area occupied by the PKH67 signal over the total cell area, defined by the dLNGFR membrane signal, and then expressed as percentage values. Co-localization analyses were performed by measuring the Manders' coefficient30 with the ImageJ plugin JaCoP, reporting the fraction of mCh^+ or $PKH67^+$ area overlapping with the selected endocytosis marker/tracer-positive area.

Flow cytometry

Flow cytometry used a LSR2 device (BD Bioscience); in all experiments, the fluorescence of GFP, mCh and mTq was directly detected using the 488-525/50, 450-450/50 and 561-610/20 channels, respectively. The full list of primary antibodies used for flow cytometry is reported in Supplementary Table 3.

Flow cytometry of iBMM and DC cultures

After cell culture, iBMMs were detached with trypsin/EDTA, whereas DCs were detached by pipetting. For dLNGFR and B2M analysis, the cells were stained with directly conjugated primary antibodies (see Supplementary Table 3 for details) in the presence of blocking solution. For F(ab)2 analysis, the cells were stained with a directly conjugated anti-F(ab)2 antibody (see Supplementary Table 3 for details) without other antibodies. The cells were finally resuspended in 7AAD-containing wash solution to exclude dead cells.

For EV treatment studies, iBMMs were seeded in 24-well plates (10^5/well) and DCs in 96-well plates (2 x 10^4/well). Cells were incubated with 2 x 10^8 EVs/well (according to NTA analysis), except where indicated otherwise. iBMMs were detached with trypsin/EDTA, whereas DCs were detached by pipetting; the cells were then washed with a mild acid solution (50 mM acetic acid, Sigma) to remove EVs attached to the cell membrane. Before flow cytometry analysis of PKH67, mCh or mTq fluorescence, the cells were stained with an APC-conjugated anti-dLNGFR antibody in the presence of Fc block. For H-2Kb staining, the cells were incubated with PE-conjugated anti-H-2Kb and APC-conjugated anti-dLNGFR antibodies, in the presence of Fc block (see Supplementary Table 3 for details). The cells were finally resuspended in 7AAD-containing wash solution to exclude dead cells.

Flow cytometry of cancer cell lines

After cell culture, cancer cells were detached with trypsin/EDTA. For B2M, H-2Kb, HER2 and GD2 staining, the cells were stained with directly conjugated primary antibodies (see Supplementary Table 3 for details) in the presence of Fc block. Before analysis, the cells were resuspended in 7AAD-containing wash solution.

Flow cytometry of EVs

To analyze HER2 on EVs, we used 10^9-10^{10} EVs in 100 μl of PBS containing an AlexaFluor-647–conjugated anti-HER2 antibody in the presence of Fc block. After 15 min at 4°C, the preparations were washed and the EVs isolated by ultracentrifugation, as described above. EVs were resuspended in PBS and analyzed using an LSR2 device (BD Bioscience).

Isolation of $CD8^+$ OT-I cells

$CD8^+$ OT-I cells were isolated from OT-I TCR transgenic mice, which produce MHC class I-restricted, ovalbumin (OVA)-specific $CD8^+$ T cells31. The spleens were collected under sterile conditions, smashed and filtered by using gravity-driven 70 μm cell strainers to obtain single cell suspensions. We depleted $CD11c^+$ cells with anti-CD11c microbeads (Miltenyi Biotech) and an autoMACS Pro separator apparatus. Subsequently, we positively selected

Europe PMC Funders Author Manuscripts

$CD8^+$ T cells using anti-CD8 microbeads (Miltenyi Biotech). $CD8^+$ T cells were maintained in RPMI medium complemented with FBS, L-glutamine and penicillin-streptomycin, non-essential amino acid solution (Sigma), sodium pyruvate (1 mM, Gibco) and 2-mercaptoethanol (25 μM, Gibco).

OT-I cell proliferation assays

$CD8^+$ OT-I cells were stained with CellTrace-violet (Life Technologies) following the manufacturer's instructions. One-2 x 10^5 $CD8^+$ OT-I cells were co-cultured in flat-bottom 96-well plates with 1-2 x 10^4 DCs. In the experiment shown in Figure 1f, DCs were pre-incubated for 24 h with EV-HER2/OVA (or control EV-OVA), washed extensively with PBS, and then added to the OT-I cells (day zero). In other experiments, DCs and T cells were incubated with EVs concomitantly (day zero). Unless indicated otherwise, 10^8-10^9 EV-particles were employed in each cell culture. In all experiments, the proliferation of $CD8^+$ OT-I cells was measured at day 3 by flow cytometry, by gating and analyzing $CD8^+7AAD^-$ T cells.

Generation of B2m and H2kb knockout MC38 cells

MC38, MC38-OVA and MC38-HER2/OVA cells were transduced with CRISPR/CAS9 LVs expressing gRNA targeting either *B2m* or *H2kb*. Forty-eight hours after transduction, the cells were cultured in IMDM medium complemented with FBS, L-glutamine, penicillin-streptomycin, puromycin (10 μg/ml, Sigma) and doxycycline (10 μg/ml, Sigma) for 4 days. The cells were then plated at a concentration of 0.5 cell/well in 96-well plates in normal cell culture medium to isolate cell clones. Cell colonies showing no expression of B2M or H-2Kb by flow cytometry were expanded and employed in experiments.

OVA DNA analysis

Genomic DNA was extracted from MC38 cells either untransduced or transduced with the CRISPR/CAS9 LVs, using the DNeasy Blood & Tissue Kit (Qiagen). OVA sequences were amplified by PCR using the following primers:

OVA_Fw: TTGCCAGTGGGACAATGAGC

OVA_Rv: GTTGGTTGCGATGTGCTTGAT

Mouse studies

Mice employed in this study were maintained in a pathogen-free barrier animal facility according to the Swiss regulations for animal care and experimental research. OT-I TCR transgenic mice were available at EPFL. C57Bl6/J, FVB/n and Nod SCID gamma (NSG) mice were purchased from Charles River Laboratory (L'Arbresle, France). All studies were performed according to protocols approved by the Swiss authorities (protocols 3154 and 2916).

DC vaccination of tumor-bearing mice

MC38-HER2 and MC38-HER2/OVA tumors were generated by injection of 1x10^6 cells subcutaneously into the right flank of 6-week old C57Bl6/J mice. In both experiments, DC

vaccinations were performed at day 7 and 14 post-tumor challenge via peritumoral injection of 10^6 DCs in 100 µl of PBS (or PBS alone as control). The volume of MC38-HER2 tumors was determined by caliper measurements and calculated using the formula: volume = $\pi/6$ x d x D^2, where d is the shorter and D the longer tumor axis. MC38-HER2/OVA tumors regressed spontaneously after a short-lived growth phase, so tumor volume data could not be considered reliable.

Analysis of OVA-specific T cells in tumor-bearing mice

To analyze OVA-specific T cells in MC38-HER2/OVA tumor-bearing mice, the mice were euthanized at day 19 post-tumor injection. After isolation and processing of the spleen (see above), single-cell suspensions were stained for 30 min with OVA-specific MHCI dextramer-APC (Immudex) diluted at 1:2, and subsequently stained with lineage-specific conjugated antibodies for 15 min at 4°C. The $CD8^+$ OT-I cells were identified as dextramer $^+CD45^+CD11b^-$ $CD4^-CD8^+7AAD^-$ cells.

Tumor/DC co-mingling assay

Transduced DCs (10^6 cells) of FVB/n origin (H-2Kb-negative) were embedded in 200 µl of matrigel (BD Bioscience) together with *H2kb* wild-type or knockout MC38-HER2/OVA cells (10^6 cells). The matrigel was supplemented with 0.5 µg of bFGF, 0.5 µg of GM-CSF (both from Peprotech) and 0.25 µg of sphingosine-1-phosphate (Cayman Chemical). Matrigel plugs containing cancer cells and DCs were then implanted subcutaneously in the flank of 8 week-old female NSG mice, which do not express H-2Kb; the matrigel implant sustains the growth of tumor-forming cancer cells in association with the co-mingled DCs. In this setting, only the *H2kb* wild-type cancer cells express H-2Kb.

The tumor implants were harvested 8 days post-injection (a time window that enabled recovering sufficient numbers of transduced DCs for analysis) and processed for flow cytometry. Briefly, the matrigel implants were excised and made into single-cell suspensions by collagenase IV (0.2 mg/ml, Worthington), dispase (2 mg/ml, Life Technologies) and DNaseI (0.1 mg/ml, New England BioLabs) treatment in IMDM medium. After 30 min at 37°C in a shaking thermoblock, the cell suspensions were filtered and washed in PBS containing 2 mM EDTA and 2% FBS. Matrigel-derived cell suspensions were incubated with conjugated antibodies against H-2Kb and cell-specific markers (see Supplementary Table 3 for details) in blocking solution. Before flow cytometry, the cells were resuspended in DAPI to exclude dead cells.

Statistics and reproducibility

Information on the study outline and sample size is presented in the main text, methods, figures and figure legends. For experiments involving cell cultures aimed to analyze cell behavior, such as T-cell proliferation or cell-binging assays, we used 2 or 3 independent cell cultures per condition. In these cases, each cell culture was regarded as a biological replicate and statistics were derived when at least 3 independent cell cultures were analyzed per condition. In other cases, we analyzed the variability of defined cellular parameters (for example, the intracellular localization of internalized EVs) at the single cell level. In these

cases, individual cells were regarded as independent biological replicates and statistics were derived when at least 8 independent cells were analyzed per condition.

Studies involving mice were performed once. Each study was designed to use the minimum number of mice required to obtain informative results (that is, quantitative data amenable to statistical analysis). No specific statistical tests were used to predetermine the sample size; our previous experience with subcutaneous tumor models provided guidance. Tumor-bearing mice were randomized before treatment by allocating mice bearing tumors ranked by volume to alternate treatment groups. We further verified that the mean tumor volume before treatment was comparable in the different experimental groups.

Experiments were not performed blinded, however, data acquisition was blinded in most of the cases. No data were excluded from analysis. Detailed information about the statistical methods is indicated in each figure legend. For comparison between two experimental groups, we applied an unpaired two-sided Student's t-test. When multiple groups were compared, we applied a one-way ANOVA analysis with either Dunnett's correction, for comparing multiple groups to a specific control group within a dataset, or Tukey's correction, for multiple comparisons within a dataset. We applied a two-way ANOVA followed by either Tukey's correction for multiple comparisons or Sidak's correction for two comparisons. Error bars show the standard error of the mean (SEM). The number and type of replicates for each experiment is indicated in the figure legends.

Data availability

Source data for all the graphical representations reported in the manuscript have been provided in Supplementary Table 2. All other data supporting the findings of this study are available from the corresponding authors on request.

A Life Science Reporting Summary for this publication is available.

Supplementary Material

Refer to Web version on PubMed Central for supplementary material.

Acknowledgements

We are grateful to G. Guarda (University of Lausanne, UNIL, Switzerland) for providing BM cells of *B2m*-deficient mice; N. Haynes (Peter MacCallum Cancer Center, Melbourne, Australia) for MC38-OVA cells; A. Ribas (University of California, Los Angeles, CA) for SM1-OVA cells; A. Donda, J.-P. Mach, and D.E. Speiser (UNIL) for valuable scientific advice; A. Lombardo (Vita-Salute San Raffaele University, Milan, Italy) for advice with CRISPR LVs; A. Royant (Institut de Biologie Structurale, Grenoble, France) for providing the mTq sequence; L. Trusolino (University of Torino Medical School, Italy) for providing the *HER2* sequence; D. Thompson and L. Giesbrecht for technical help; and the EPFL core facilities of flow cytometry (FCCF), proteomics (PCF), and bioimaging/optics platform (BIOp), for skillful assistance. S.K.H. was supported by the Swiss Federal Commission for Scholarships for Foreign Students (Swiss Government Excellence Scholarship 2015.0430). This study was funded by grants from the European Research Council (ERC-CoG EVOLVE), the EPFL Catalyze4Life program, and the Swiss National Foundation (SNF grant 31003A-165963) to M.D.P.

References

1. Simons M, Raposo G. Exosomes--vesicular carriers for intercellular communication. Current opinion in cell biology. 2009; 21:575–581. [PubMed: 19442504]

2. Tkach M, Thery C. Communication by Extracellular Vesicles: Where We Are and Where We Need to Go. Cell. 2016; 164:1226–1232. [PubMed: 26967288]
3. Becker A, et al. Extracellular Vesicles in Cancer: Cell-to-Cell Mediators of Metastasis. Cancer cell. 2016; 30:836–848. [PubMed: 27960084]
4. Bobrie A, Thery C. Exosomes and communication between tumours and the immune system: are all exosomes equal? Biochemical Society transactions. 2013; 41:263–267. [PubMed: 23356294]
5. Wolfers J, et al. Tumor-derived exosomes are a source of shared tumor rejection antigens for CTL cross-priming. Nature medicine. 2001; 7:297–303.
6. Zhang B, Yin Y, Lai RC, Lim SK. Immunotherapeutic potential of extracellular vesicles. Frontiers in immunology. 2014; 5:518. [PubMed: 25374570]
7. Gu X, Erb U, Buchler MW, Zoller M. Improved vaccine efficacy of tumor exosome compared to tumor lysate loaded dendritic cells in mice. International journal of cancer. Journal international du cancer. 2015; 136:E74–84. [PubMed: 25066479]
8. Arteaga CL, et al. Treatment of HER2-positive breast cancer: current status and future perspectives. Nature reviews. Clinical oncology. 2011; 9:16–32.
9. Amendola M, Venneri MA, Biffi A, Vigna E, Naldini L. Coordinate dual-gene transgenesis by lentiviral vectors carrying synthetic bidirectional promoters. Nature biotechnology. 2005; 23:108–116.
10. Squadrito ML, et al. Endogenous RNAs modulate microRNA sorting to exosomes and transfer to acceptor cells. Cell reports. 2014; 8:1432–1446. [PubMed: 25159140]
11. Hogquist KA, et al. T cell receptor antagonist peptides induce positive selection. Cell. 1994; 76:17–27. [PubMed: 8287475]
12. Dolan BP, Gibbs KD Jr, Ostrand-Rosenberg S. Dendritic cells cross-dressed with peptide MHC class I complexes prime CD8+ T cells. Journal of immunology (Baltimore, Md. : 1950). 2006; 177:6018–6024.
13. Wakim LM, Bevan MJ. Cross-dressed dendritic cells drive memory CD8+ T-cell activation after viral infection. Nature. 2011; 471:629–632. [PubMed: 21455179]
14. Joffre OP, Segura E, Savina A, Amigorena S. Cross-presentation by dendritic cells. Nature reviews Immunology. 2012; 12:557–569.
15. Ludigs K, et al. NLRC5 shields T lymphocytes from NK-cell-mediated elimination under inflammatory conditions. Nature communications. 2016; 7:10554.
16. Ahmed M, Cheung NK. Engineering anti-GD2 monoclonal antibodies for cancer immunotherapy. FEBS letters. 2014; 588:288–297. [PubMed: 24295643]
17. Groux-Degroote S, Guerardel Y, Delannoy P. Gangliosides: Structures, Biosynthesis, Analysis, and Roles in Cancer. Chembiochem : a European journal of chemical biology. 2017
18. Baer C, et al. Suppression of microRNA activity amplifies IFN-gamma-induced macrophage activation and promotes anti-tumour immunity. Nature cell biology. 2016; 18:790–802. [PubMed: 27295554]
19. Palucka AK, Coussens LM. The Basis of Oncoimmunology. Cell. 2016; 164:1233–1247. [PubMed: 26967289]
20. Zhou H, et al. Structural insights into the down-regulation of overexpressed p185(her2/neu) protein of transformed cells by the antibody chA21. The Journal of biological chemistry. 2011; 286:31676–31683. [PubMed: 21680730]
21. Squadrito ML, et al. miR-511-3p modulates genetic programs of tumor-associated macrophages. Cell reports. 2012; 1:141–154. [PubMed: 22832163]
22. Amendola M, Venneri MA, Biffi A, Vigna E, Naldini L. Coordinate dual-gene transgenesis by lentiviral vectors carrying synthetic bidirectional promoters. Nature biotechnology. 2005; 23:108–116.
23. Horwacik I, et al. Structural Basis of GD2 Ganglioside and Mimetic Peptide Recognition by 14G2a Antibody. Molecular & cellular proteomics : MCP. 2015; 14:2577–2590. [PubMed: 26179345]
24. Goedhart J, et al. Structure-guided evolution of cyan fluorescent proteins towards a quantum yield of 93%. Nature communications. 2012; 3:751.

25. Squadrito ML, et al. Endogenous RNAs modulate microRNA sorting to exosomes and transfer to acceptor cells. Cell reports. 2014; 8:1432–1446. [PubMed: 25159140]

26. Leto SM, et al. Sustained Inhibition of HER3 and EGFR Is Necessary to Induce Regression of HER2-Amplified Gastrointestinal Carcinomas. Clinical cancer research : an official journal of the American Association for Cancer Research. 2015; 21:5519–5531. [PubMed: 26296355]

27. Koller BH, Marrack P, Kappler JW, Smithies O. Normal development of mice deficient in beta 2M, MHC class I proteins, and CD8+ T cells. Science. 1990; 248:1227–1230. [PubMed: 2112266]

28. De Palma M, Naldini L. Transduction of a gene expression cassette using advanced generation lentiviral vectors. Methods in enzymology. 2002; 346:514–529. [PubMed: 11883088]

29. Chopra T, et al. Quantitative mass spectrometry reveals plasticity of metabolic networks in Mycobacterium smegmatis. Molecular & cellular proteomics : MCP. 2014; 13:3014–3028. [PubMed: 24997995]

30. Dunn KW, Kamocka MM, McDonald JH. A practical guide to evaluating colocalization in biological microscopy. American journal of physiology. Cell physiology. 2011; 300:C723–742. [PubMed: 21209361]

31. Hogquist KA, et al. T cell receptor antagonist peptides induce positive selection. Cell. 1994; 76:17–27. [PubMed: 8287475]

Europe PMC Funders Author Manuscripts

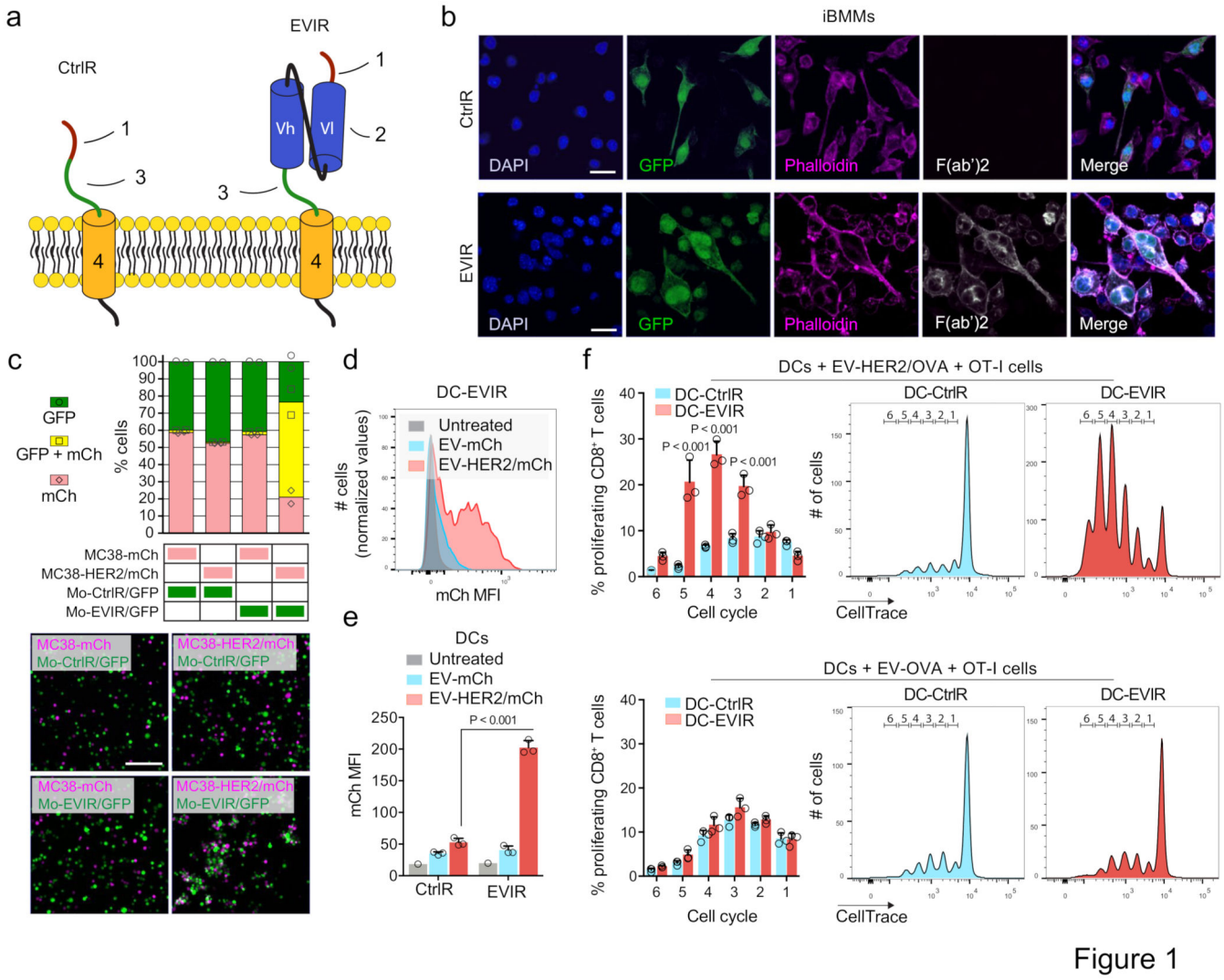

Figure 1. An anti-HER2 EVIR promotes tumor EV uptake and antigen presentation by DCs

(**a**) Schematic representation of CtrlR (left) and EVIR (right) on the cell membrane. The extracellular domain comprises an IgK signal peptide (1), a scFv domain (2; only present in the EVIR), and a hinge domain (3). The hinge domain and the transmembrane/intracellular domain (4) are derived from a non-signaling, truncated dLNGFR.

(**b**) Representative confocal images showing nuclear staining with DAPI (blue), direct GFP fluorescence (green), actin fibers stained with phalloidin (magenta), and anti-scFv immunostaining (white), in iBMM-CtrlR and anti-HER2 iBMM-EVIR cells. The cells were analyzed 7 days post-transduction. Scale bar, 50 μm. One cell culture *per* LV type is shown; data are representative of 3 independent cell cultures.

(**c**) Cell suspension binding assay using Mo-EVIR/GFP (or control Mo-CtrlR/GFP) and MC38-HER2/mCh (or control MC38-mCh) cells at 1:1 ratio. The cells were incubated in suspension for 20 min. The upper panel shows the proportion of cells that appear either as single cells (green or salmon pink, representing monocytes and MC38 cells, respectively) or in clusters (yellow, representing monocytes bound to MC38 cells), according to flow

Europe PMC Funders Author Manuscripts

cytometry analysis. The bottom panels show representative images of MC38 cells (mCh^+, magenta) and monocytes (GFP^+, green), transduced as indicated and imaged before flow cytometry; scale bar, 200 μm. Data in the top panel indicate mean values of two independent cell cultures *per* condition.

(**d**) Flow cytometry analysis of mCh in DC-EVIR either untreated or treated with EV-mCh or EV-HER2/mCh. Data are representative of 3 independent cell cultures *per* condition.

(**e**) Median fluorescence intensity (MFI) of mCh in DC-CtrlR and DC-EVIR either untreated or treated with EV-mCh or EV-HER2/mCh. Data indicate mean values ± SEM (n=3 independent cell cultures *per* condition); statistical analysis by two-way ANOVA with Sidak's multiple comparison test.

(**f**) Flow cytometry analysis of $CD8^+$ OT-I cell proliferation assessed by CellTrace dilution after their co-culture with DC-CtrlR or DC-EVIR cells exposed to EV-OVA or EV-HER2/OVA. The left panels show the percentage of $CD8^+$ OT-I cells that have completed a defined number of cell cycles (1 to 6). Data show mean percentages ± SEM (n=3 independent cell cultures *per* condition); statistical analysis by two-way ANOVA with Sidak's multiple comparison test. The middle and right panels show representative flow cytometry histograms (one cell culture of 3 performed *per* condition).

Numerical values for the experiments with quantitative data are presented in Supplementary Table 2.

Europe PMC Funders Author Manuscripts

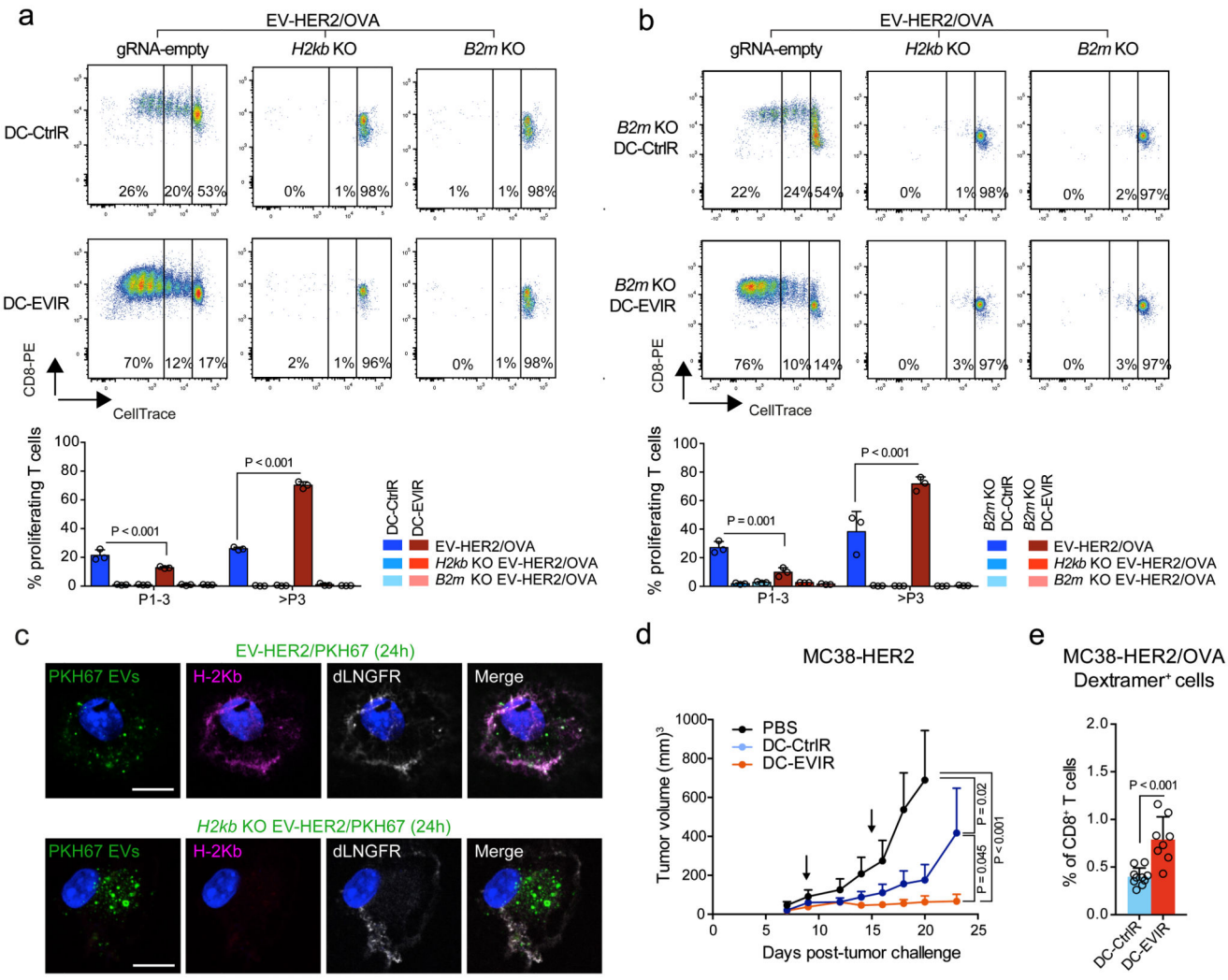

Figure 2. An anti-HER2 EVIR cross-dresses DCs with EV-derived MHCI/antigen complexes and enhances the anti-tumoral capacity of DC vaccination in mice

(**a-b**) Flow cytometry analysis of $CD8^+$ OT-I cell proliferation assessed by CellTrace dilution after co-culture with DCs and EVs, as indicated. The top panels show representative flow cytometry dot plots. The bottom panels show the percentages of $CD8^+$ OT-I cells, which completed 1 to 3 (P1-3) or more than 3 (P>3) cell cycles. Data show mean percentage values ± SEM (n=3 independent cell cultures *per* condition); statistical analysis by two-way ANOVA with Tukey's multiple comparison test.

(**c**) H-2Kb-negative DC-EVIR obtained from FVB/n mice were incubated with PKH67-labelled (green), *H2kb* wild-type (top panels) or KO (bottom panels) EV-HER2 and analyzed after 24 h. The cells were stained with antibodies to reveal H-2Kb (magenta) and dLNGFR (white). Nuclei are stained with DAPI (blue). Scale bar, 10 μm. Images are representative of 10 cells *per* condition; additional representative images are shown in Supplementary Figure 10. Data are representative of 2 independent cell culture experiments.

(**d**) Volume of subcutaneous MC38-HER2 tumors in mice vaccinated with two sequential DC infusions, indicated by the arrows. Data show mean tumor volume ± SEM (PBS, n=4

mice; DC-CtrlR, n=7; DC-EVIR, n=9). Statistical analysis by two-way ANOVA with Tukey's multiple comparison test. The experiment was performed one time.

(**e**) Flow cytometry analysis showing the percentage of OVA-specific (dextramer+) $CD8^+$ T cells in the spleens of MC38-HER2/OVA tumor-bearing mice vaccinated with DCs as indicated. Data show mean percentages ± SEM (DC-CtrlR, n=10 mice; DC-EVIR, n=8); statistical analysis by two-tailed unpaired Student's t test. The experiment was performed one time.

Numerical values for the experiments with quantitative data are presented in Supplementary Table 2.

Europe PMC Funders Author Manuscripts